Article

Structural, Magnetic and Mossbauer studies of Transition metal doped $Gd_2Fe_{16}Ga_{0.5}TM_{0.5}$ intermetallic compounds (TM=Cr, Mn, Co, Ni, Cu, and Zn)

J. N. Dahal [1,3,*], K. S. Syed Ali[2], and J. Alam[1]

1. Department of Physics, The University of Memphis, Memphis, TN 38152, USA
2. Department of Science, Harmony Science Academy, 12005 Forestgate Dr. Dallas, TX 75243, USA
3. Department of Physics, Georgia Southern University, Savannah GA 31419, USA

Abstract: The effect of transition metal substitution for Fe and the structural and magnetic properties of $Gd_2Fe_{16}Ga_{0.5}TM_{0.5}$ (TM=Cr, Mn, Co, Ni, Cu, and Zn) compounds were investigated. Rietveld analysis of X-ray diffraction indicates that all the samples crystallize in the hexagonal Th_2Ni_{17} structure. The lattice parameters: a, c and unit cell volume show TM ionic radii dependence. Both Ga and TM atoms show preferred site occupancy for 12*j* and 12*k* sites. The saturation magnetization at maximum room temperature was observed for Co, Ni, and Cu of 69, 73, and 77 emu/g, respectively while minimum value was observed for Zn (62emu/g) doping $Gd_2Fe_{16}Ga_{0.5}TM_{0.5}$. Highest Curie temperature of 590K was observed for Cu doping which is 15% and 5% and higher than Gd_2Fe_{17} and $Gd_2Fe_{16}Ga$ compounds, respectively. The hyperfine parameters viz. hyperfine field and isomer shift, show systematic dependence on the TM atomic number. The observed magnetic and Curie temperature behavior in $Gd_2Fe_{16}Ga_{0.5}TM_{0.5}$ is explained on the basis of Fe(3d)-TM(3d) hybridization. The superior Curie temperature and magnetization value of Co, Ni, and Cu doped $Gd_2Fe_{16}Ga_{0.5}TM_{0.5}$ compounds as compared to pure Gd_2Fe_{17} or $Gd_2Fe_{16}Ga$ makes $Gd_2Fe_{16}Ga_{0.5}TM_{0.5}$ a potential candidate for high-temperature industrial magnet applications.

Keywords: Permanent magnetic materials; 2:17 intermetallics; Mossbauer Spectroscopy; Curie temperature; X-ray diffraction; Rietveld analysis

Preprints (www.preprints.org) | NOT PEER-REVIEWED | Posted: 4 October 2018 doi:10.20944/preprints201810.0075.v1

1. In.troduction

The rare-earth intermetallic compounds R_2Fe_{17} have energy product (BH)max and Hc to be about 26 MGOe and 15 kOe, respectively [1]. In spite of these properties, they exhibit low Curie temperature (Tc). For example, 473 K for Gd_2Fe_{17} and 300 K for Dy_2Fe_{17} along with low magnetic anisotropies [2]. Various strategies have been employed addressing issues related to improving magnetic anisotropy, magnetization and Curie temperature of R_2Fe_{17} compounds. Metalloids such as C, N, and H atoms are added to improve the magnetic anisotropy and Curie temperature [3,4,5,6]. However, high-temperature processing of these interstitial modified compounds is difficult. Subsequently, the addition of non-magnetic atoms such as Al, Ga, and Si for iron in the $R_2Fe_{17-x}M_x$ compound was investigated which in fact showed Curie temperature enhancement at high non-magnetic atom content. Among Al, Si, and Ga, Ga substituted compounds show high Tc, e.g., $Sm_2Fe_{16}Ga$, Tc ~485 K [7] and $Dy_2Fe_{16}Ga$, Tc~462 K [8]. However, this improvement in Tc is overshadowed by a concomitant deterioration in saturation magnetization as iron atoms are being replaced by non-magnetic atoms.

The Curie temperatures T_C in the R_2Fe_{17} compounds was explained on the base of strength of exchange interaction between Fe-Fe pairs [9]. It is based on the assumption that the exchange interactions favor ferromagnetic (r>rc) or antiferromagnetic (r<rc), where r_C ~2.5 Å. Hence, Tc is assumed dependent on the competition between ferromagnetic and antiferromagnetic exchange interactions between neighboring pairs of Fe-Fe ions located at various crystallographic positions. This means that Tc enhancement can be achieved via unit cell lattice expansion, except in Si-substituted $RE_2Fe_{17-x}Si_x$, favoring ferromagnetic exchange interaction between Fe-Fe pairs. Usually, such lattice expansion is possible either via substituting for Fe ions by ions with the larger ionic radii [10,11] or via insertion of interstitial atoms in the unit cell [12,13]. It was observed that there are two ingredients influencing T_C value: local magnetic moment values and exchange interaction values [14].

Among R_2Fe_{17} intermetallic, Gd_2Fe_{17} is of special interest as it has the highest Curie temperature, T_C. Among the doped $R_2Fe_{17-x}M_x$ (M=Al. Si. Ga), Ga doped compounds display higher Tc value [**15**]. Given the above, the present work investigates effect of doping transition metal (TM) atoms in Ga doped $Gd_2Fe_{16}Ga_{0.5}TM_{0.5}$ compounds and compare the results with Gd_2Fe_{17}. It is expected that the doping of TM atoms with ionic radii greater than Fe will bring unit cell volume expansion and hence improve Fe-Fe exchange interaction enough to couple Fe-Fe moments ferromagnetically; thus, improving

 doi:10.20944/preprints201810.0075.v1

the Curie temperature of the compound. Furthermore, there also lies the possibility of improving magnetic moment of Fe via Fe-TM 3d band hybridization which can either bring band narrowing or increase exchange splitting by moving the 3d↑ states below the Fermi level or allow charge transfer out of the 3d band, provided the spin-down density of states exceed the spin-up density [16].

This study discusses the changes in the structural and magnetic properties in R_2Fe_{17} compounds when Fe is substituted in $R_2Fe_{16}Ga_{0.5}TM_{0.5}$ compounds with transition metal TM = Cr, Mn, Co, Ni, Cu, and Zn. The main aim of the study is to bring structural and band related changes to R_2Fe_{17} compounds such as to improve Tc without impacting the saturation magnetization.

2. Experimental

The raw materials of Gd, Fe, Ga and TM (TM=Cr, Mn, Co, Ni, Cu, and Zn) with 99.9% purity were purchased from Sigma Aldrich. The parent alloys $Gd_2Fe_{16}Ga_{0.5}TM_{0.5}$ were prepared by arc melting the stoichiometric amount of aforementioned elements under a high purity argon atmosphere. The ingots were melted several times to ensure the high degree of homogeneity.

XRD was carried out with CuK_α (λ~1.5406 Å) radiation on a Bruker (D8 Advance) diffractometer. The powder X-ray data sets were collected in the 2θ range from 20° to 75° with a step size of 0.042°. The XRD analysis was performed by the well-known structural refinement Rietveld [17] method using the JANA2006 [18] software package to fit the experimental and calculated diffraction patterns. The initial crystal structure parameters were used as given by Liao et al. [19]. In the hexagonal setting, Gd was fixed at the 2*b* and 2*d* site (0, 0, 0.25) and (0.333, 0.667, 0.75), Fe is fixed at 4*f*, 6*g*, 12*j*, and 12*k* (0.333 0.667 0.105), (0.5 0 0), (0.333 0.969 0.25), and (0.167 0.333 0.985). The profile was constructed using a pseudo-Voigt function. Profile asymmetry was introduced by employing the multi-term Simpson rule integration devised by Howard [20]. A surface roughness correction was also applied using the Pitschke, Hermann, and Matter [21] model. In this technique, structural parameters, lattice parameters, peak shift, background profile shape and preferred orientation parameters are used to minimize the difference between a calculated profile and the observed data.

Magnetic properties of the powder sample were investigated at room temperature using vibrating sample magnetometer (VSM) in the maximum field of 1.2T. In order to minimize

Preprints (www.preprints.org) | NOT PEER-REVIEWED | Posted: 4 October 2018 doi:10.20944/preprints201810.0075.v1

the effect of demagnetizing field, the samples were compacted at 3000psi and cut into rectangular parallelepiped with the ratio of length to a width larger than three times and embedded in epoxy. Modified thermogravimetric analyzer (DuPont 910) equipped with a permanent magnet was used to determined Curie temperature of composite samples. In this procedure, a magnetic material is placed inside an empty, tared TGA pan located near a strong magnet. The material is then heated. At the Curie temperature (Tc), the magnetic properties disappear (i.e., the material goes from diamagnetic to paramagnetic) and the reduced attraction for the magnet results in a sharp apparent weight loss or gain (depending on the TGA design).

The Mossbauer spectra of the samples were obtained at room temperature (RT) using a 25 mCi ^{57}Co source in an Rh foil mounted on a constant acceleration drive system (SEE Co. Minneapolis, USA) in transmission geometry. The velocity scale of the Mossbauer spectrometer was calibrated by measuring the hyperfine field of α-Fe foil, at room temperature. The Mossbauer spectra were analyzed using WMoss software from SEE Co. The spectra were least-square fitted with the hyperfine field (f&f), isomer shift (IS) and quadrupole splitting (QS) as variables.

3. Results and Discussion

The raw powder profile for $Gd_2Fe_{16}Ga_{0.5}TM_{0.5}$ systems is presented in **Fig. 1 (a)**. The inset **Fig. 1(a)**, the enlarged 2θ view between 41.5° – 43.3°, shows that there is a shift in 2θ towards the lower angle which indicates the expansion of the unit cell with the substitution of increasing atomic number of TM in the compound. This observation is in accordance with the increasing size of the substitution atom whose metallic radii increase as going from TM=Cr to Zn, **Table I**. The refined Rietveld profiles are presented in Fig. 1(b) for $Gd_2Fe_{16}Ga_{0.5}TM_{0.5}$ systems. The refined structural parameters, lattice parameters *a*, *c*, *c/a* ratio, unit cell volume and the reliability indices are given in **Table I**. From the Rietveld analysis, the refined profile indicates that $Gd_2Fe_{16}Ga_{0.5}TM_{0.5}$ compounds crystallize in hexagonal Th_2Ni_{17} structure with $P6_3/mmc$ symmetry group. **Fig. 2** show the lattice parameters a function of TM atomic number in $Gd_2Fe_{16}Ga_{0.5}TM_{0.5}$. It is observed from **Fig.2** that the variation in lattice parameter *a* is more pronounced than that in *c* in doped compounds. This is also evident from the variation in *c/a* ratio (**Table I**), which indicates anisotropic expansion of unit cell volume with TM atom doping. The doping of, Cr up to Co, brings lattice contraction while Ni, Cu, and Zn brings in lattice expansion. The observed trend in lattice parameter closely follows TM metallic radii, **Fig. 2**.

Preprints (www.preprints.org) | NOT PEER-REVIEWED | Posted: 4 October 2018 doi:10.20944/preprints201810.0075.v1

Table 1: Structural parameters from Rietveld refinement of powder XRD data of $Gd_2Fe16Ga_{0.5}TM_{0.5}$ (TM= Cr, Mn, Fe, Co, Ni, Cu, Zn, and Ga) with Gd_2Fe_{17}.

Parameter	*Cr*	*Mn*	Gd_2Fe_{17} Fe	Co	Ni	Cu	Zn	$Gd_2Fe_{16}Ga$ Ga
Metallic radii (pm)	127	126	129	125	125	128	136	140
a (Å)	8.5149(43)	8.5267(42)	8.4791(21)	8.4911(81)	8.4812(24)	8.4997(32)	8.5435(52)	8.5555(61)
c (Å)	8.3320(32)	8.3521(22)	8.3326(6)	8.3421(8)	8.3338(32)	8.3451(16)	8.3641(62)	8.3682(33)
c/a	0.9785	0.9795	0.9827	0.9824	0.9826	0.9818	0.9790	0.9781
Cell Volume ($Å^3$)	526.97	527.32	522.2634	525.15	523.60	526.06	528.21	528.5749
R_{obs} (%)	5.67	4.44	2.48	4.53	3.21	3.99	2.31	6.43
wR_{obs} (%)	4.32	5.21	3.55	5.31	4.21	4.87	3.65	7.12
R_p (%)	6.22	7.87	9.12	8.11	7.32	7.22	5.32	10.55
wR_p (%)	7.87	8.86	10.54	9.32	8.32	10.11	7.78	12.54

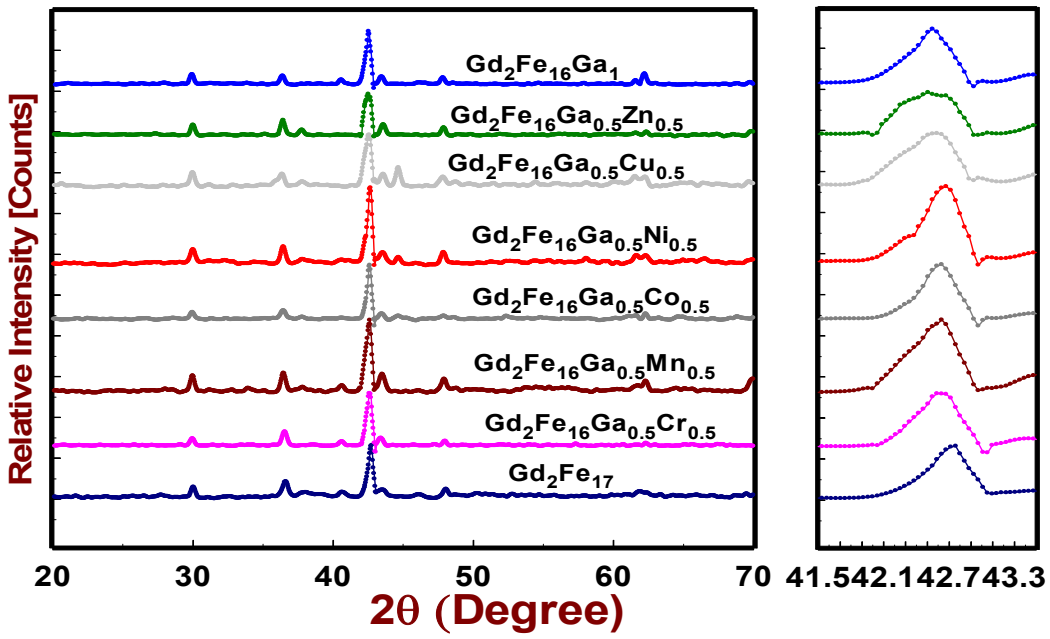

Figure 1 (a) : Raw XRD powder profile for $Gd_2Fe_{16}Ga_{0.5}TM_{0.5}$ (TM = Cr, Mn, Co, Ni, Cu, Zn, and Ga) with Gd_2Fe_{17}.

Preprints (www.preprints.org) | NOT PEER-REVIEWED | Posted: 4 October 2018 doi:10.20944/preprints201810.0075.v1

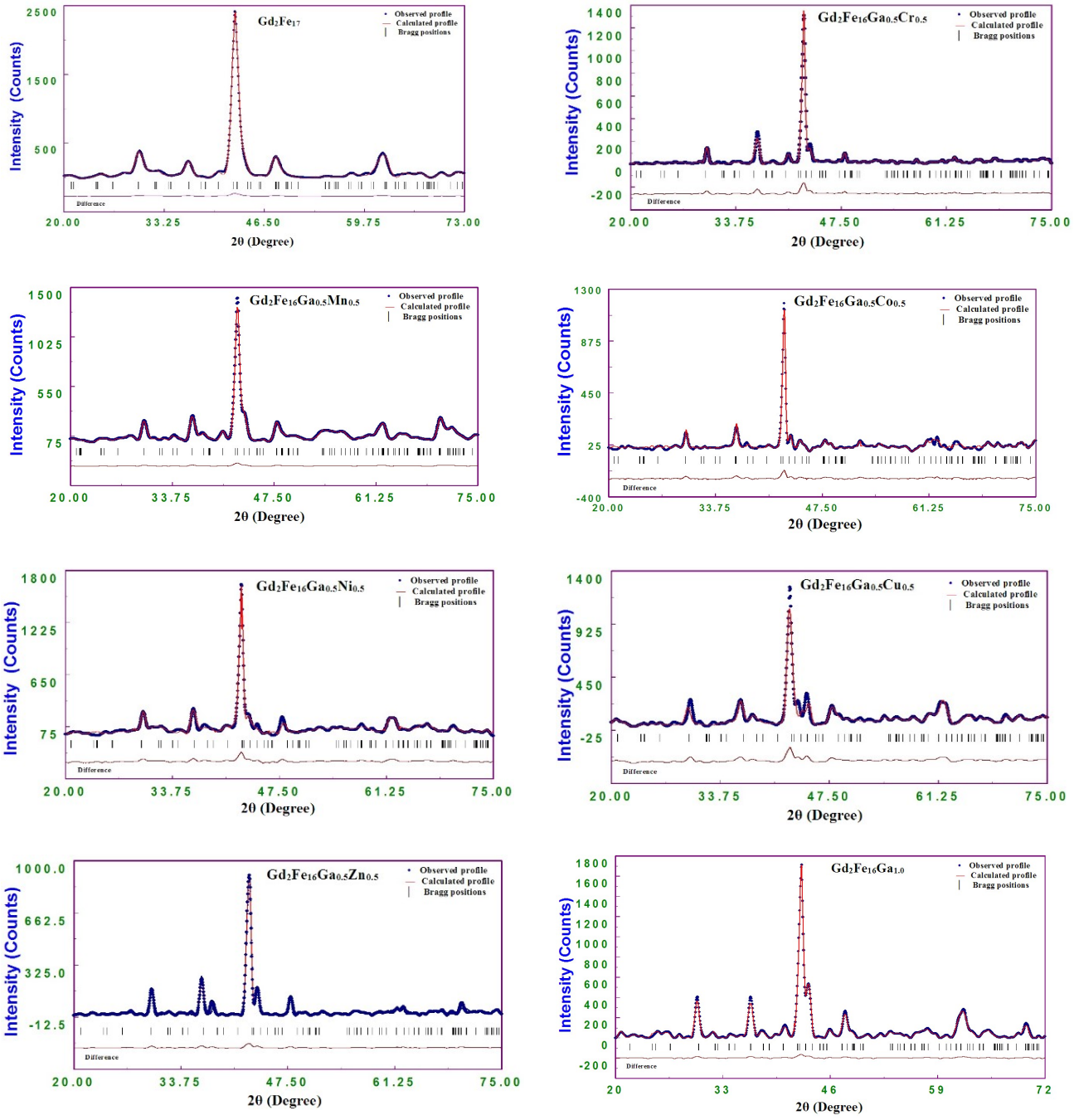

Figure 1(b): Rietveld refined XRD data of $Gd_2Fe_{16}Ga_{0.5}TM_{0.5}$ (TM = Cr, Mn, Co, Ni, Cu, Zn, and Ga) with Gd_2Fe_{17}.

Preprints (www.preprints.org) | NOT PEER-REVIEWED | Posted: 4 October 2018 doi:10.20944/preprints201810.0075.v1

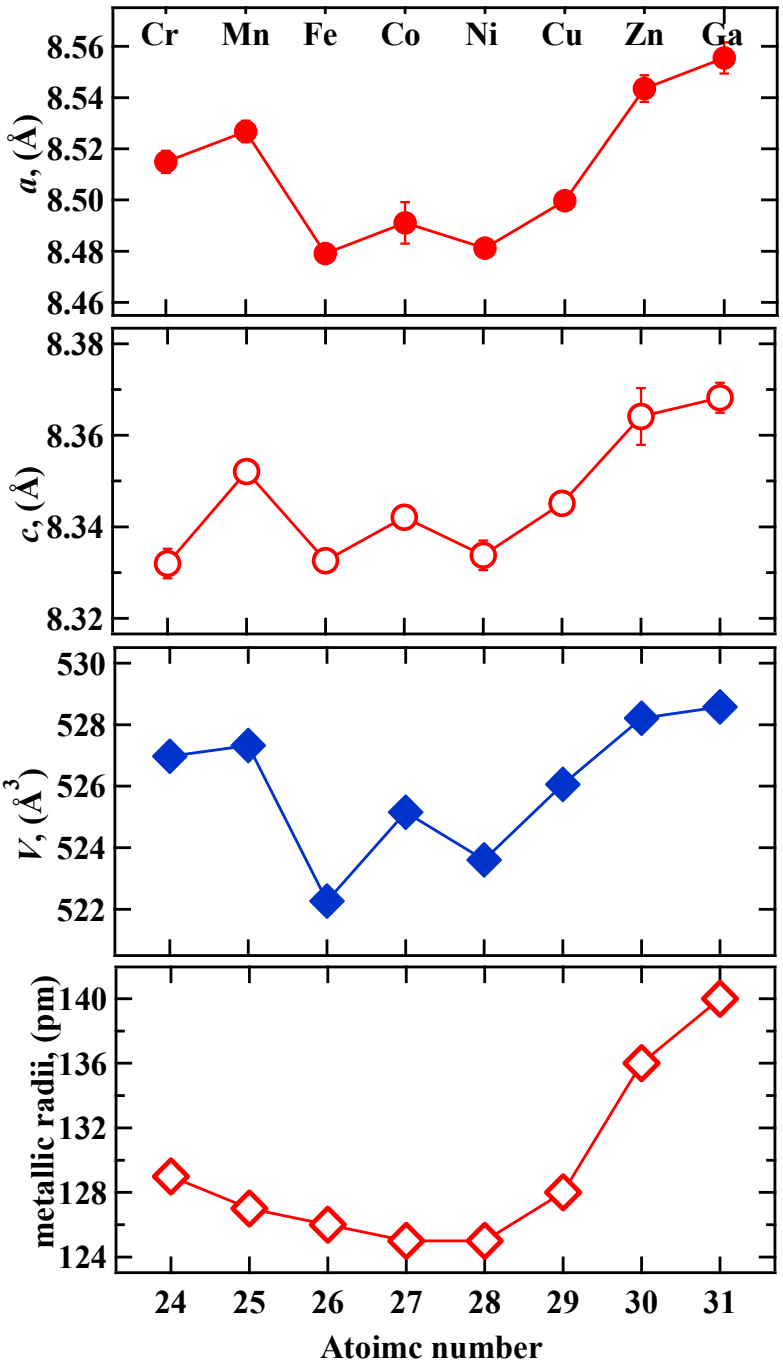

Figure 2: Lattice parameters, derived via Rietveld refinement, and metallic radii of $Gd_2Fe_{16}Ga_{0.5}TM_{0.5}$ as a function of TM atomic number.

The atomic site occupancy for Gd, Fe, Ga and TM atoms derived from Rietveld refinement is listed in **Table II**. The site notations are given for rhombohedral structure with

Preprints (www.preprints.org) | NOT PEER-REVIEWED | Posted: 4 October 2018 doi:10.20944/preprints201810.0075.v1

corresponding hexagonal notation viz. 6*c*(4*f*), 9*d*(6*g*), 18*f*(12*j*) and18h(12*k*). The crystallographic site preference exhibited by TM in $Gd_2Fe_{16}Ga_{0.5}TM_{0.5}$ is listed in **Table II**. It is evident from **Table II** that Ga prefers 12*j* and 12*k* sites to other sites, while TM avoids 4*f* sites and prefers to remain closer to Ga at 12*j* and 12*k* sites. The TM atoms display the occupancy preference in order of 12j~12k>6g>4f. Thus, the 6*c* (4*f*) dumbbell site is the least affected by the TM substitution. Results of site occupancy are in close conformity with the previous Neutron diffraction [22,23] and ^{57}Fe Mossbauer studies [24,25,26] on $R_2Fe_{17-x}Ga_x$ where Ga atoms preferentially occupy mainly the 18*h*(12*k*) site in the Th_2Zn_{17} structure for x<4. The number of Fe and R nearest neighbors (NN) for Fe atoms at various crystallographic sites in R_2Fe_{17} compounds is as follow; at Fe 6c site (dumbbell site) there are 13 Fe NN and 1 R NN, at Fe 9d site there are 10 Fe NN and 2 R NN, at Fe 18f there are 10 Fe NN and 2 R NN, and at Fe 18h site there are 9 Fe NN and 3 R NN. In addition, the Wigner-Seitz cell volume is follows 6*c*(4*f*)>18*h* (12*k*)>18*f*(12*j*)> 9*d*(6*g*) trend. The marked preference of Ga and TM atoms for 12*j* and 12*k* sites suggest that the Ga affinity for R atoms surpasses the Wigner-Seitz site volume [**15**].

Table II: Atomic site occupancy derived from Rietveld refinement for $Gd_2Fe_{16}Ga_{0.5}TM_{0.5}$ (TM = Cr, Mn, Co, Ni, Cu, Zn, Ga) with Gd_2Fe_{17}.

TM	*Gd1(2b)*	*Gd2(2d)*	*Fe(4f)*	*Fe(6g)*	*Fe(12j)*	*Fe(12k)*	*Ga(4f)*	*Ga(6g)*	*Ga(12j)*	*Ga(12k)*	*TM(4f)*	*TM(6g)*	*TM(12j)*	*TM(12k)*
Cr	0.0861	0.0809	0.1581	0.2360	0.4580	0.4956	0.0047	0.0068	0.0148	0.0112	0.0072	0.0032	0.0159	0.0181
Mn	0.0829	0.0846	0.1510	0.2327	0.4379	0.5017	0.0042	0.0061	0.0128	0.0108	0.0082	0.0041	0.0166	0.0188
Fe	0.0854	0.0815	0.1706	0.2580	0.4973	0.5293								
Co	0.0835	0.0827	0.1509	0.2410	0.4589	0.4891	0.0057	0.0118	0.0112	0.0115	0.0047	0.0093	0.0144	0.0157
Ni	0.0861	0.0809	0.1518	0.2527	0.4323	0.4824	0.0081	0.0117	0.0062	0.0171	0.0069	0.0103	0.0147	0.0162
Cu	0.0839	0.0821	0.1503	0.2435	0.4521	0.4803	0.0052	0.0121	0.0118	0.0109	0.0051	0.0083	0.0151	0.0169
Zn	0.0816	0.0839	0.1511	0.2321	0.4310	0.4956	0.0045	0.0058	0.0124	0.0102	0.0075	0.0042	0.0179	0.0129
Ga	0.0812	0.0836	0.1455	0.2314	0.4285	0.4863	0.0094	0.01938	0.0309	0.0341				

The Fe-Fe site-to-site bond distances are listed in **Table III** and are plotted in **Fig. 3.** It is observed from the **Table III**, that the 4*f*-4*f* bond distances are smallest (~2.40 Å) and 12*k*-12*k* (2.46 Å) and 12*j*-12*j* (2.57 Å) distances are greatest of all. Other bond distances such as 6*g*-12*j*, 6*g*-12*k* and 12*k*-12*k* have values close to 2.45 Å and do not show much variation with TM doping. It is to be noted that because of the aforementioned variation in bond distances, it is highly unlikely that these bond-length changes will have a drastic effect on

Preprints (www.preprints.org) | NOT PEER-REVIEWED | Posted: 4 October 2018 doi:10.20944/preprints201810.0075.v1

the Curie temperature of the compounds. In fact, a slight reduction in bond-distances is observed up to Cu substitution, which ideally should lead to increase in antiferromagnetic exchange coupling between Fe-Fe moments and hence Curie temperature reduction. The observed changes in bond-distances are in-line with the metallic radii of the TM atoms, **Figure 2.**

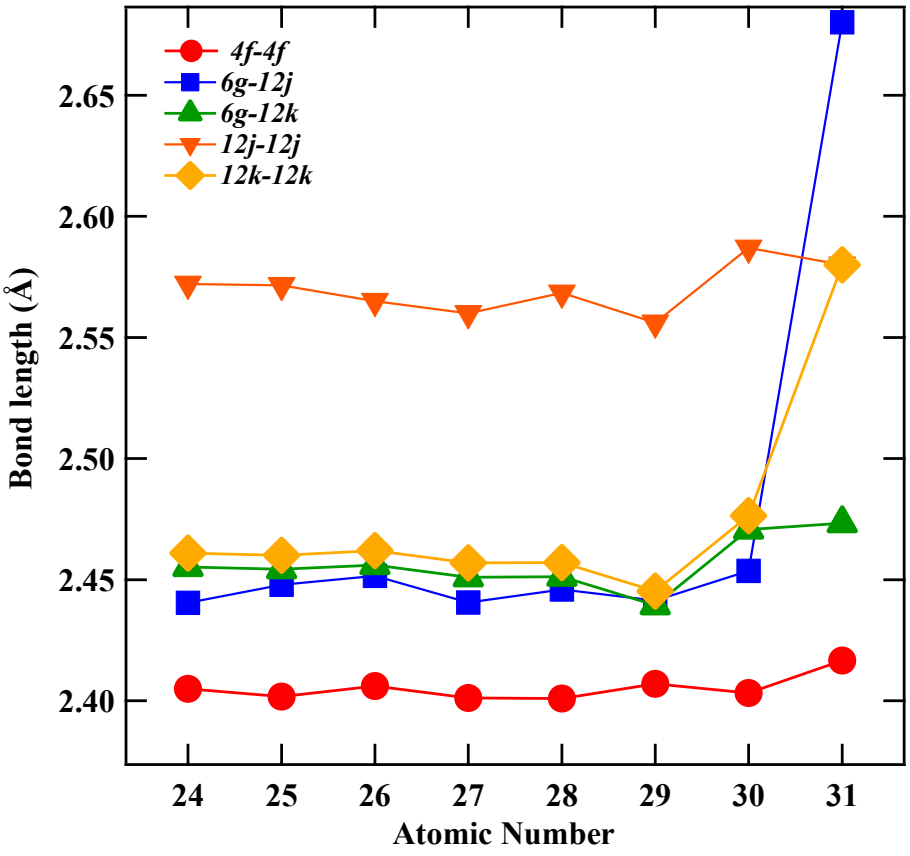

Figure 3: Atomic site-site bond lengths as a function of TM atomic number in $Gd_2Fe_{16}Ga_{0.5}TM_{0.5}$ (TM = Cr, Mn, Co, Ni, Cu, Zn, and Ga) with Gd_2Fe_{17}.

Preprints (www.preprints.org) | NOT PEER-REVIEWED | Posted: 4 October 2018 doi:10.20944/preprints201810.0075.v1

Table III: Interatomic Fe–Fe distances (in Å) for $Gd_2Fe_{16}Ga_{0.5}TM_{0.5}$ (TM = Cr, Mn, Co, Ni, Cu, Zn, and Ga) with Gd_2Fe_{17}.

Fe-Fe sites	*C r*	*Mn*	*Fe*	*Co*	*Ni*	*Cu*	*Zn*	*Ga*
4f-4f	2.4050(4)	2.4018(13)	2.4061(3)	2.4012(5)	2.4010(11)	2.4070(3)	2.4032(2)	2.4166(21)
6g-12j	2.4405(9)	2.4479(9)	2.4516(2)	2.4406(16)	2.4460(3)	2.4414(7)	2.4536(3)	2.6801(3)
6g-12k	2.4552(13)	2.4543(5)	2.4560(2)	2.4510(7)	2.4513(3)	2.4394(11)	2.4707(2)	2.4734(3)
12j-12j	2.5721(3)	2.5715(2)	2.5650(1)	2.5600(7)	2.5684(2)	2.5561(2)	2.587(21)	2.5800(3)
12k-2k	2.4610(13)	2.4600(13)	2.4620(4)	2.4570(2)	2.4571(11)	2.4453(11)	2.4764(11)	2.5800(12)

Room temperature magnetization vs. field plot for $Gd_2Fe_{16}Ga_{0.5}TM_{0.5}$is shown in **Fig. 4**. The room temperature magnetic parameters derived from VSM are plotted in **Fig. 5** and are listed in **Table IV**. The Law of Approach to Saturation, $M = M_s(1 - A/H - B/H^2) + \chi^*H$ was used to determine the saturation magnetization. The last term is the forced magnetization term. A is a constant correlated with the contribution of micro-stress/inclusions, and B is a constant correlated with magneto-crystalline anisotropy. Where magneto-crystalline is dominant term, a plot of M vs. $1/H^2$ in the high field region gives a straight line, the intercept of which (with the M-axis) gives the saturation magnetization and the slope of which gives the magneto-crystalline anisotropy constant. Interesting variation in saturation magnetization, Ms, is noticed with the TM atom doping. The Ms was observed to decrease first with Cr and Mn doping and then increase with TM atomic number up to Cu and then decreased for Zn and Ga doping. Highest Ms ~77 emu/g was observed with Cu doping in $Gd_2Fe_{16}Ga_{0.5}TM_{0.5}$. While low saturation magnetization was observed upon Cr (60 emu/g), Mn (57 emu/g), and Zn (59 emu/g) doping. As compared to Gd_2Fe_{17} (67 emu/g), $Gd_2Fe_{16}Ga_{0.5}Cu_{0.5}$ (77 emu/g) showed an increase of 15% in Ms value. The observed variation in Ms can be attributed to the F(3d)-TM (3d) hybridization effect of orbitals. The extent of Fe(3d)-3d hybridization raises or lowers the bandwidth, which eventually changes the magnetic moment of Fe atoms [27,28]. The electronic configuration of Cr ($[Ar]4s^13d^5$, Mn $[Ar]4s^23d^5$, Fe $[Ar]4s^23d^6$, Co $[Ar]4s^23d^7$, Ni $[Ar]4s^23d^8$, Cu $[Ar]4s^13d^{10}$, Zn $[Ar]4s^23d^{10}$ and Ga $[Ar]\ 4s^2\ 4p^13d^{10}$). In case of early transition metals, 3d states are positioned at higher energies than those of Fe. Due to exchange splitting 3d↓ spin-down states have moved up in energy, and therefore close to the 3d states of early transition metals. Thus, the hybridization of 3d states of early transition metals is stronger with 3d↓ spin-down states than 3d↑ spin-up states of Fe. As a result, the fraction of spin down 3d↓ states of early transition metals found in the energy region of Fe 3d is increased. Since the Fermi level is

Preprints (www.preprints.org) | NOT PEER-REVIEWED | Posted: 4 October 2018 doi:10.20944/preprints201810.0075.v1

situated in this region, anti-ferromagnetic coupling follows. For the late transition metals, the situation is reversed and ferromagnetic coupling follows [29,30,31]. In view of this explanation, Cr, and Mn-doped $Gd_2Fe_{16}Ga_{0.5}TM_{0.5}$ show lower magnetization while Co, Ni, and Cu doped samples show increasingly higher magnetization. A rather rapid decrease in Ms has been reported in $Er_2Fe_{17-x}Mn_x$ with increasing Mn content, which has been attributed to the antiferromagnetic coupling between Fe and Mn [32]. The lower magnetization values of Zn and Ga results from the magnetic dilution effect upon replacing magnetic Fe with non-magnetic Zn and Ga.

Table IV: Room temperature saturation magnetization and Curie temperature of $Gd_2Fe_{16}Ga_{0.5}TM_{0.5}$ (TM = Cr, Mn, Co, Ni, Cu, Zn, and Ga) with Gd_2Fe_{17}.

$Gd_2Fe_{16}Ga_{0.5}TM_{0.5}$	Ms(emu/gm)	Tc (K)
Cr	59.78	571
Mn	56.75	526
Gd_2Fe_{17}.	67.00	513
Co	68.61	587
Ni	72.61	557
Cu	76.79	570
Zn	59.04	537
$Gd_2Fe_{16}Ga_1$	67.49	559

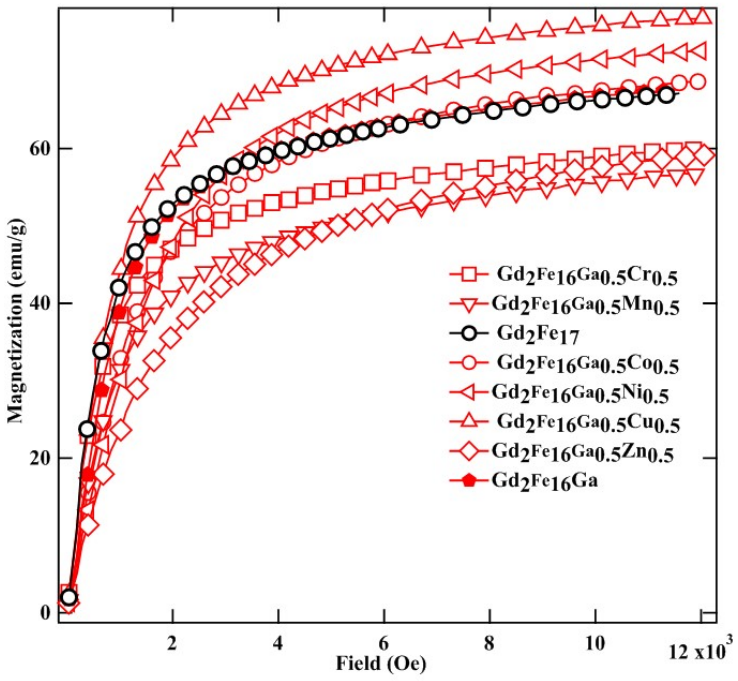

Figure 4: Room temperature M vs. H of $Gd_2Fe_{16}Ga_{0.5}TM_{0.5}$ (TM = Cr, Mn, Co, Ni, Cu, Zn, and Ga) with Gd_2Fe_{17}.

Preprints (www.preprints.org) | NOT PEER-REVIEWED | Posted: 4 October 2018 doi:10.20944/preprints201810.0075.v1

The measured Curie temperature, Tc, of $Gd_2Fe_{16}Ga_{0.5}TM_{0.5}$ compounds is plotted in **Fig. 5** as a function of TM atomic number. It is evident from **Fig.5** that the TM doping affects the Tc of $Gd_2Fe_{16}Ga_{0.5}TM_{0.5}$ compounds. The Curie temperature reaches a maximum value of 587 K for Co doping followed by a reduction in Tc with increasing TM atomic number. A 15% increase in Tc was observed upon Co doping in $Gd_2Fe_{16}Ga_{0.5}TM_{0.5}$ as compared to that of Gd_2Fe_{17} (513 K) and a 4% increase as compared to $Gd_2Fe_{16}Ga$ (559K). In the Fe-rich R_2Fe_{17} intermetallics, the Tc is mainly determined by the strength and number of Fe-Fe exchange interactions. The strength of Fe-Fe exchange interaction is strongly dependent on the interatomic Fe-Fe distances described [9,33,34,35]. Accordingly, the exchange interactions between iron atoms situated at distances smaller (greater) than 2.45−2.50 Å are negative (positive). In the R_2Fe_{17} majority of Fe-Fe distances favor the negative interaction [36]. The negative exchange interaction can be reduced either by volume expansion or by reducing the number of Fe-Fe pairs with negative exchange interactions. The low T_C observed in parent Gd_2Fe_{17} compound is believed to be due to the short Fe–Fe interatomic distances found at the 4*f*(6*c*) sites in the hexagonal (rhombohedral) structure which couple antiferromagnetically since their separation is ~2.4 Å, **Fig. 3**, which is less than 2.45 Å needed for ferromagnetic ordering [37]. It is to be noted that increase in Tc has been reported earlier with higher Al, Ga, and Si content (at x>2) in $R_2Fe_{17-x}M_x$ (M=Al, Ga, Si) [**15**] however with a concomitant reduction in Ms due to large Fe replacement with non-magnetic atoms. A Tc value of 581 K has been reported earlier in $YGdFe_{16}CoGa$ [**38**] compound but reported Tc~586 K of $Gd_2Fe_{16}Ga_{0.5}Co_{0.5}$ exceeds that of the former compounds. Thus, the observed increase in Tc in TM doped $Gd_2Fe_{16}Ga_{0.5}TM_{0.5}$ compounds is highest with a minimum replacement of Fe atoms.

Preprints (www.preprints.org) | NOT PEER-REVIEWED | Posted: 4 October 2018 doi:10.20944/preprints201810.0075.v1

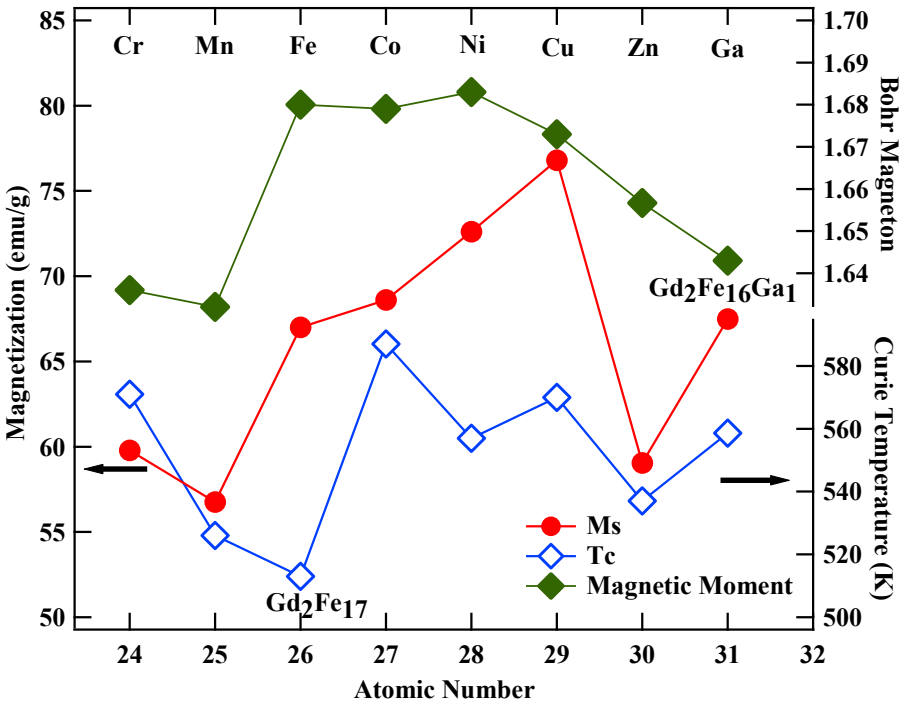

Figure 5: Saturation magnetization, Curie temperature, and Bohr magneton number as a function of atomic number in $Gd_2Fe_{16}Ga_{0.5}TM_{0.5}$ (TM = Cr, Mn, Co, Ni, Cu, Zn, and Ga) with Gd_2Fe_{17}.

Friedel model [39] can also be used to explain the observed variation in Tc. According to this model the strength of interaction between two magnetic moments would be strong and ferromagnetic, if $\lambda/d>1$, where distance "d" between these magnetic atoms is smaller than the distance " λ" covered by the main peak of the Friedel oscillations. In compounds containing 3d transition metals, it has been established that the magnetic coupling is governed mainly by the nearest-neighbor interactions and is proportional to the lattice parameters. Furthermore, λ is found to be inversely proportional to the Fermi wave vector, k_f. For the 3d band in the R_2Fe_{17} compounds, k_f is large. Substitution of TM decreases the holes in the 3d band and hence decreases k_f. The substitution of Ga leads to lattice expansion and hence increases "d", which will have an effect of reducing λ/d ratio. Since the substitution of Co, Ni and Cu brings in lattice volume reduction as compared to $R_2Fe_{16}Ga$; there is hence an increase in the, $\lambda/d>1$ and Tc [37,38]. The reported theoretical studies attribute changes in the Curie temperature in substituted $R_2Fe_{17-x}T_x$ (T=Al, Si, Ga, and Ti) intermetallics to be electronic in origin other than due to the simple volume expansion effect and hence bond-distances [40,41,42]. The effect of the substitution is to

Preprints (www.preprints.org) | NOT PEER-REVIEWED | Posted: 4 October 2018 doi:10.20944/preprints201810.0075.v1

fill out the Fe-3d spin-up sub-bands which alter the magnetic moment of the compound and hence the strength of exchange interaction [39,43]. In fact, theoretical calculations performed using LSDA+U method showed that enhancement between Fe-Fe atoms in the presence of Ga in $Gd_2Fe_{17-x}Ga_x$ compounds, which intern was shown to enhance Curie temperature for low Ga ($x<3$) content [44]. Thus, observed higher Tc values of $Gd_2Fe_{16}Ga_{0.5}TM_{0.5}$ as compared to that of pure Gd_2Fe_{17} could be attributed to this effect as well. In comparison to various doped intermetallics such as $Gd_2Fe_{16}Ga$ (~410 K) [45], $Gd_2Fe_{16}Ga_{0.5}Ti_{0.5}$ (556 K) [46], $Dy_2Fe_{16}Ga$ (~462K) [8], $Ce_2Fe_{16}Ga$ (~320K) [47], $Sm_2Fe_{16}Ga$ (~505K) [48], or $Sm_2Fe_{16.2}Ti_{0.8}$ (~435K) [49], the reported compound $Gd_2Fe_{16}Ga_{0.5}TM_{0.5}$ with Co, Ni, and Cu substitution certainly exhibits higher Tc and Ms, thus ensuring their potential use as high temperature permanent magnet applications.

The room temperature (RT) Mossbauer spectra for $Gd_2Fe_{16}Ga_{0.5}TM_{0.5}$ are shown in **Fig. 6**. The R_2Fe_{17} intermetallics with Th_2Ni_{17} structure, have the easy direction of magnetization and hyperfine field lying in the basal plane along *a* or *b* axes of the unit cell [50,51]. This basal plane easy direction of magnetization complicates the Mossbauer spectral analysis of R_2Fe_{17} compounds because it involves four crystallographically inequivalent iron sites. The reason for the inequivalent iron site is the vector character of the hyperfine field and tensor character of the electric field gradient [52]. Thus, this inequivalency demands further magnetic splitting of g, *j,* and *k* iron sites. Mössbauer studies of $Gd_2Fe_{16}Ga_{0.5}TM_{0.5}$ have been conducted accordingly, either with 8 or 10 magnetic sextets, with absence or presence of impurity phase, respectively [46,53,54,55]. The Mössbauer spectral analysis was carried out with magnetic sextets assigned to the 4*f*, 6*g*, 12*j*, and 12*k* sites in Gd_2Fe_{17}. The 6g, 12*j,* and 12*k* sites were further split into 2, 3, and 2 corresponding to the site occupancies of Fe atoms in the crystal structure of R_2Fe_{17} with the planar anisotropy. The intensities of the six absorption lines of each sextet were assumed to follow the 3:2:1 intensity ratio expected for randomly oriented powder samples in zero magnetic field and a single common line-width was assumed for all the eight sextets. The isomer shifts (IS,δ) for the magnetically inequivalent sites were constrained to be the same, whereas the hyperfine field (HF, B_{hf}) were expected to vary at pairs of magnetically inequivalent sites due to variations in the dipolar and orbital contributions to the magnetic hyperfine fields [56]. The ^{57}Fe Mossbauer spectra show hyperfine split sextets in $Gd_2Fe_{16}Ga_{0.5}TM_{0.5}$ revealing that the samples are magnetically ordered and all of them have different subspectra with different magnetic hyperfine fields.

 doi:10.20944/preprints201810.0075.v1

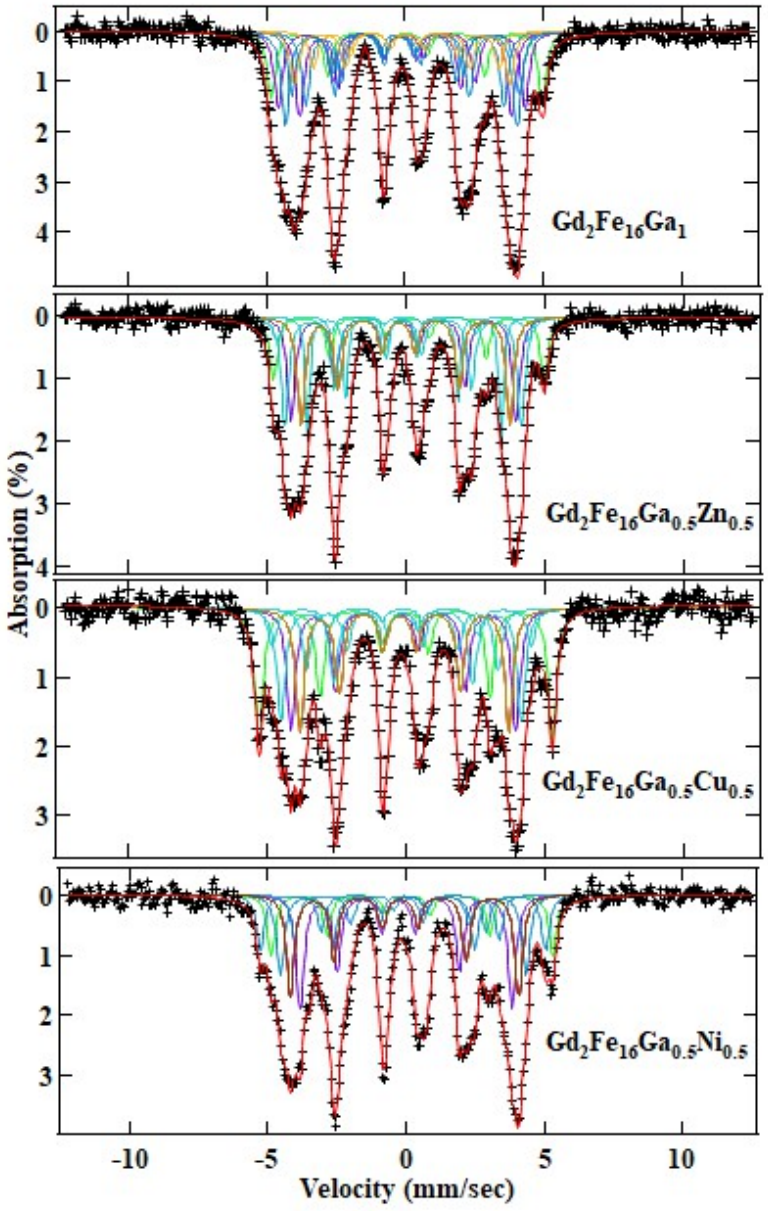

Preprints (www.preprints.org) | NOT PEER-REVIEWED | Posted: 4 October 2018 doi:10.20944/preprints201810.0075.v1

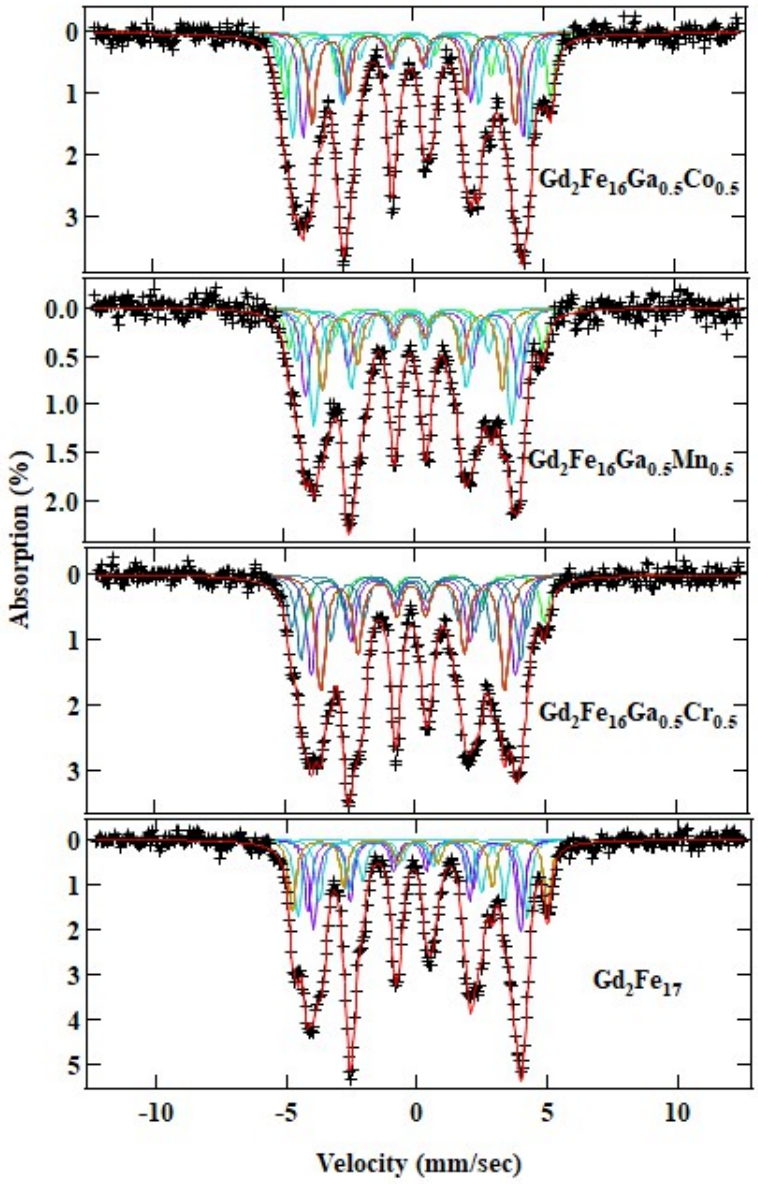

Figure 6: Fitted room temperature Mossbauer spectra of $Gd_2Fe_{16}Ga_{0.5}TM_{0.5}$ (TM = Cr, Mn, Co, Ni, Cu, Zn, and Ga) with Gd_2Fe_{17}.

The hyperfine parameters derived from the fitting are listed in **Table V**, and weighted average (Wt.Avg.) hyperfine field (HF) and isomer shifts (IS, δ) are plotted in **Fig. 7**. There exists a direct correlation between hyperfine field values of a site to its near neighbor (NN) iron sites. In case of Th_2Ni_{17} structure, 12*k* site has 9 NN Fe sites (1 (4*f*), 2 (6*g*), 4 (12*j*), 2(12*k*)), *12j* has 10 NN Fe sites (2 (4*f*), 2 (6*g*), 2 (12*j*), 4 (12*k*)), 6*g* has 10 NN Fe sites (2 (4*f*), 0 (6*g*), 4 (12*j*), 4(12*k*)), and 4*f* site has 11 NN Fe sites (1 (4*f*), 3 (6*g*), 6 (12*j*), 3 (12*k*)). Following the NN distribution, the observed HF values are in *4f(6c)>12j(18f)>6g(9d)>12k(18h)* sequence, which is similar to the sequence observed in

Preprints (www.preprints.org) | NOT PEER-REVIEWED | Posted: 4 October 2018 doi:10.20944/preprints201810.0075.v1

other R_2Fe_{17} compounds [57,58]. It is obvious that 4*f* (6*c*) site has the maximum hyperfine field, since it has the maximum number of Fe nearest neighbors, whereas, the 18*h* (12*k*) site has the minimum number of Fe neighbors and consequently has the least HF value. Although 6*g*(9*d*) and 12*j*(18*f*) sites have the same number of Fe neighbors, the former has comparatively smaller Fe-Fe distances and hence a larger hyperfine field, **Table III** and **Table V**. The Cu and Mn-doped $Gd_2Fe_{16}Ga_{0.5}TM_{0.5}$ display a low Wt. Avg. HF values as compared to other TM doped $Gd_2Fe_{16}Ga_{0.5}TM_{0.5}$ compounds. The Wt. Avg. HF value reaches the maximum for Gd_2Fe_{17} and $Gd_2Fe_{16}Ga_{0.5}Co_{0.5}$, to a value ~252 kOe followed with a gradual decline in its value, reaching to a value of 246 kOe for $Gd_2Fe_{16}Ga_1$. This decrease in HF value results from the decreased magnetic exchange interactions resulting from Fe replacement with non-magnetic Cu, Zn, and Ga atoms. Furthermore, under the first approximation, the hyperfine field is assumed proportional to the magnetic moment. We obtained the Fe moment using the hyperfine coupling constant of 150 kOe/μB, which has been reported for Y–Fe systems [59,60]. The average value of Fe magnetic moment for $Gd_2Fe_{16}Ga_{0.5}TM_{0.5}$ is plotted in **Fig. 5**. In general, Fe magnetic moment holds up to the value of 1.68 μ_B only for Fe, Co, and Ni substitution in $Gd_2Fe_{16}Ga_{0.5}TM_{0.5}$.

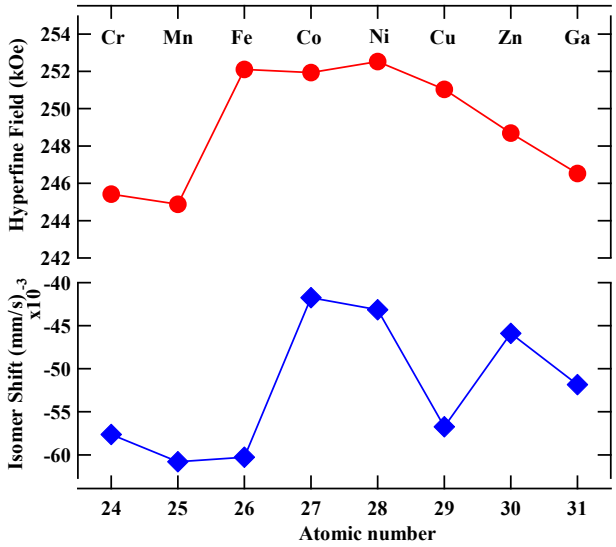

Figure 7: Weighted average hyperfine parameters viz. Hyperfine field and Isomer shift, as a function of atomic number for $Gd_2Fe_{16}Ga_{0.5}TM_{0.5}$ (TM = Cr, Mn, Co, Ni, Cu, Zn, and Ga) with Gd_2Fe_{17}.

 doi:10.20944/preprints201810.0075.v1

1 **Table V**: RT Mossbauer hyperfine parameters for $Gd_2Fe_{16}Ga_{0.5}TM_{0.5}$ (TM = Cr, Mn, Co, Ni, Cu, Zn, and Ga) with Gd_2Fe_{17}.

TM		4*f*	6g_1	6g_2	12j_1	12j_2	12j_3	12k_1	12k_2	*Doublet*	Wt. Avg.
Cr	B(Koe)	303	231.6	244.1	212.5	271.2	278.5	198	255.3		245.424
	IS(mm/s)	0.102	-0.121	-0.121	-0.1	-0.1	-0.1	0.011	0.011		-0.0576
	QS(mm/s)	0.351	0.116	0.162	0.073	-0.157	-0.009	0.35	-0.0446		
	A(%)	10	15.2	17.8	12.5	4.3	18.5	9.9	11.7		
Mn	B(Koe)	302.3	230	254.3	210.1	265.2	275.1	202	255.6		244.882
	IS(mm/s)	0.078	-0.117	-0.117	-0.124	-0.124	-0.124	0.039	0.039		-0.0608
	QS(mm/s)	0.28	0.093	0.093	-0.157	0.149	-0.079	0.434	-0.17		
	A(%)	8.2	16.3	17.6	8.7	23.1	10.6	10.7	6.2		
(Gd_2Fe_{17})	B(Koe)	304	246.2	254.6	220.5	272.3	286.3	205.6	260.2		252.1
	IS(mm/s)	0.07	-0.13	-0.13	-0.115	-0.115	-0.115	0.035	0.035		-0.0603
	QS(mm/s)	0.067	0.296	0.21	-0.019	0.009	-0.116	0.358	-0.487		
	A(%)	13.8	15.5	19.8	6.1	13.6	11.9	6.16	11.7		
Co	B(Koe)	315.2	242.7	262.9	215.6	271.3	283	203.2	264.6		251.932
	IS(mm/s)	0.11	-0.119	-0.119	-0.098	-0.098	-0.098	0.056	0.056		-0.0417
	QS(mm/s)	0.139	0.272	0.238	-0.399	0.015	-0.039	0.263	-0.245		
	A(%)	11.5	16	18.1	7.1	18.4	5.9	10.1	10.8		
Ni	B(Koe)	310.1	239.1	257.4	220.6	276.7	285.2	201.9	263.3	44.4	252.524
	IS(mm/s)	0.113	-0.129	-0.129	-0.09	-0.09	-0.09	0.044	0.044	0.5	-0.0432
	QS(mm/s)	0.265	0.458	0.055	-0.036	0.042	-0.079	0.138	0.151	-0.5	
	A(%)	11	3.5	9.3	8	18.6	8.3	14.3	16.6	8.4	
Cu	B(Koe)	312.2	234.5	252.1	214.8	269.2	290.3	200.2	268	45.9	251.032
	IS(mm/s)	0.113	-0.137	-0.137	-0.128	-0.128	-0.128	0.062	0.062	0.387	-0.0567

Preprints (www.preprints.org) | NOT PEER-REVIEWED | Posted: 4 October 2018 doi:10.20944/preprints201810.0075.v1

	QS(mm/s)	0.021	0.172	0.102	-0.005	-0.083	-0.103	-0.358	-0.17	-0.39	
	A(%)	22	20.8	20.4	10.3	18.7	6.5	1.9	2.6	2.8	
	B(Koe)	303.4	234.5	252.3	217.1	265	280.7	211.3	256.4		248.689
	IS(mm/s)	0.088	-0.141	-0.141	-0.101	-0.101	-0.101	0.062	0.062		-0.0459
Zn	QS(mm/s)	0.041	0.252	0.125	0.098	-0.0001	-0.033	0.178	-0.145		
	A(%)	11.3	19.4	18.8	13.2	19.5	4.3	3.4	9.1		
	B(Koe)	304.8	235.6	238.3	222.8	255.1	283.8	208.2	252.9		246.529
	IS(mm/s)	0.059	-0.109	-0.109	-0.113	-0.113	-0.113	0.05	0.05		-0.0518
Ga	QS(mm/s)	0.025	-0.086	0.211	0.216	0.275	-0.023	0.093	-0.147		
	A(%)	12.3	14	15.3	13.5	11.7	17.3	6.8	9.9		

The isomer shift values were assigned in relation to the Wigner-Seitz cell volume, i.e. the greater the Wigner-Seitz cell volume, the greater the isomer shift, **Table V** [61]. So, as V(4*f*)>V(12*j*)~V(12*k*)>V(6*g*), their corresponding IS follow as δ4*f*>δ12*j*~δ12*k*>δ6*g*. The room temperature values of Wt. Avg. IS for $Gd_2Fe_{16}Ga_{0.5}TM_{0.5}$ are negative and the magnitudes of IS increase with increasing TM atomic number in $Gd_2Fe_{16}Ga_{0.5}TM_{0.5}$. The IS is proportional to the total *s*-electron charge density at the iron nucleus, which is the sum of the spin-up and spin-down *s*-electron density and lattice site volume; an increasing *s*-electron density at iron nucleus is indicated by a decreasing isomer shift. The observed behavior of IS value could be attributed to the competition between lattice site volume and complex nature of hybridization between Fe-Ga-TM [62,63], which all affect the *s*-electron charge density at the iron nucleus. A volume contraction is observed until TM=Ni followed with unit cell expansion till TM=Zn doping in $Gd_2Fe_{16}Ga_{0.5}TM_{0.5}$. However, the Wt. Avg. IS value becomes less negative with TM=Co and onward. Thus, this behavior of IS indicates electronic effects at play in dictating IS behavior of $Gd_2Fe_{16}Ga_{0.5}TM_{0.5}$ compound. The increased IS value for with Co, Ni, Cu, Zn, and Ga in $Gd_2Fe_{16}Ga_{0.5}TM_{0.5}$ could be associated with the increased number of the 3d electrons which increases the shielding of the *s*-electrons from the nucleus. In earlier TM atoms viz. Cr and Mn, the 3d band is broader and heavily hybridized with the conduction band [38]. These make electrons freer and thus have a greater presence at the Fe nucleus, which makes IS more negative. The increased screening of *s*-electrons via 3d electrons beyond TM=Fe doping in $Gd_2Fe_{16}Ga_{0.5}TM_{0.5}$ could be the reason for enhanced IS.

4. Conclusion

The effect of double substitution Ga and TM in $Gd_2Fe_{16}Ga_{0.5}TM_{0.5}$ on structural and magnetic properties is compared with Gd_2Fe_{17} compounds. These compounds were found to crystallize in hexagonal Th_2Ni_{17} type structure. Lattice parameters and unit cell volume of TM doped $Gd_2Fe_{16}Ga_{0.5}TM_{0.5}$ compounds show dependence on atomic radii of TM dopant. The variance of c/a ratio with the substation in these compounds show anisotropic unit cell volume expansion. The Rietveld analysis show preferred occupancy of Ga for 12*k* and 12*j* while TM for 12*k* sites. Overall, no direct correlation was observed between the trend in Curie temperature and bond-distances. In fact, the observed Tc reached a maximum value of 587 K for cobalt substitution, which is 15% higher than Tc value of Gd_2Fe_{17}. Furthermore, 15% and 14% enhancement in Ms was observed for Cu substituted

$Gd_2Fe_{16}Ga_{0.5}TM_{0.5}$ compound as compared to Dy_2Fe_{17} and $Dy_2Fe_{16}Ga_1$ compounds, respectively. Furthermore, unlike other doped compounds of $RE_2Fe_{17-x}M_x$ (M=Al, Si, Ga) intermetallics, where improvements in Tc is comprised with the reduction in Ms, in the present studied compound $Gd_2Fe_{16}Ga_{0.5}TM_{0.5}$, even small TM doping (TM=Co, Ni, and Cu) brings in a simultaneous enhancement in Ms and Tc. The combined magnetic and Mossbauer study points to the fact that the observed improvement in Tc and Ms could be attributed to electronic effects resulting from Fe-3d hybridization with substituted TM atom electronic shell. A concomitant improvement in Ms and Tc is desirable for the magnetic industry. The study elucidates that the judicious selection of dopants and its content can improve Ms and Tc of the R_2Fe_{17} intermetallic compounds.

Reference

1. N. I. LLC, "Permanent magnet selection and design handbook," Magcraft, Advance Magnetic Materials, Vienna VA, (2007).
2. K. J. Strnat, "Chapter 2 - Rare earth-cobalt permanent magnets," in *Handbook of Ferromagnetic Materials*, vol. 4, p. 131–209 (1988).
3. J. M. D. Coey and Hong Sun**, "**Improved magnetic properties by treatment of iron-based rare earth intermetallic compounds in ammonia", J. Magn. Magn. Mater. **87**, L251, (1990).
4. J. M. D. Coey, Hong Sun, Y. Otani, and D. P. F. Hurley, "Gas-phase carbonation of R_2Fe_{17}; R = Y, Sm", J. Magn. Magn. Mater. **98**, 76 (1991).
5. X. P. Zhong, R. J. Radwanski, F. R. de Boer, T. H. Jacobs, and K. H. J. Buschow," Magnetic and crystallographic characteristics of rare-earth ternary carbides derived from R_2Fe_{17} compounds", J. Magn. Magn. Mater. **86**, 333 (1990).
6. K. H. J. Buschow, R. Coehoorn, D. B. de Mooji. K. de Waard, and T. H. Jacobs, "Structure and magnetic properties of $R_2Fe_{17}N_x$ compounds", J. Magn. Magn. Mater. **92**, L35 (1990).
7. R. Xu, L. Zhen, D. Yang, J. Wu, X. Wang, Q. Wang, C. Chen and L. Dai, "Effect of Ga on the structural stablity of $Sm_2(FeGa)_{17}$ compounds," Materials letters, **57**, 146 (2002).
8. B.-G. Shen, Z.-h. Cheng, H.-y. Gong, B. Liang, Q.-w. Yan and W.-s. Zhan, "Magnetic anisotropy of $Dy_2Fe_{17-x}Ga_x$ compounds," Solid State Commun. **95**, 813 (1995).

9. D. Givord and R. Lemaire, "Magnetic transition and anomalous thermal expansion in R_2Fe_{17} compounds," IEEE Trans. Magn. MAG **10**, 109 (1974).
10. T. H. Jacobs, K. H. J. Buschow, G. F. Zhou, X. Li, and F. R. de Boer, "Magnetic interactions in $R_2Fe_{17-x}Al_x$ compounds (R = Ho, Y)", J. Magn. Magn. Mater. **116**, 220 (1992).
11. B. G. Shen, F. W. Wang, L. S. Kong, and L. Cao, **"**Magnetic anisotropy of $Sm_2Fe_{17-x}Ga_x$ compounds with 0 < or = x < or = 6", J. Phys.: Condens. Matter **5**, L685 (1993).
12. H. Sun, J. M. D. Coey, Y. Otani, and D. P. F. Hurley, "Magnetic properties of a new series of rare-earth iron nitrides: $R_2Fe_{17}N_y$(y approximately 2.6)" J. Phys.: Condens. Matter **2**, 6465 (1990).
13. D. B. de Mooij and K. H. J. Buschow, "Formation and magnetic properties of the compounds $R_2Fe_{14}C$" J. Less-Common. Met. **142**, 349 (1988).
14. A.V. Lukoyanov, E.E. Kokorina, M.V. Medvedev, and I.A. Nekrasov "Ab initio exchange interactions and magnetic properties of Gd_2Fe_{17} iron sublattice: rhombohedral vs. hexagonal phases, Phys. Rev. B, 80, 104409 (2009)
15. K. V. S. Rama Rao, H. Ehrenberg, G. Markandeyulu, U. V. Varadaraju, M. Venkatesan, K. G. Suresh, V. S. Murthy, P. C. Schmidt, and H. Fuess "On the Structural and Magnetic Properties of $R_2Fe_{17-x}(A,T)_x$ (R =Rare Earth; A Al, Si, Ga; T= Transition Metal)Compounds," phys. stat. sol. (a) **189**, 373 (2002).
16. J. M. D. Coey, "New permanent magnets; manganese compounds" J. Phys.: Condens. Matter, **26**, 064211 (2014).
17. H. M. Rietveld, "A profile refinement method for nuclear and magnetic structures" J. Appl. Cryst. **2**, 65 (1969).
18. V. Petříček, M. Dušek and L. Palatinus, "Crystallographic Computing System JANA2006: General features, Z. Kristallogr. **229,** 345 (2014).
19. L. X. Liao, Z. Altounican, and D. H. Ryan, "Cobalt site preferences in iron rare-earth-based compounds," Phy. Rev. B **47**, 11230 (1993).
20. C. J. Howard, "The approximation of asymmetric neutron powder diffraction peaks by sums of Gaussians," J. Appl. Crystallogr. **15**, 15615 (1982).

21. W. Pitschke, H. Hermann, and N. Mattern, "The influence of surface roughness on diffracted X-ray intensities in Bragg–Brentano geometry and its effect on the structure determination by means of Rietveld analysis," Powder Diff. **8**, 74 (1993).
22. Q. W. Yang, Q. W. Yan, P.L. Zhang, B. G. Shen, F. W. Lang, L. S. Kong, C. Gou, D. F. Chen, and Y. F. Cheng, "A neutron powder diffraction study of the structure of $Ho_2Fe_{17-x}Ga_xC_2$ (x=4.0 and 5.5)," J. Phys.: Condens. Mater. **6,** 3567 (1994).
23. Z. Hu, W. B. Yelon, S. Mishra, G. J. Long, O. A. Pringle, D. P. Middleton, K. H. J Buschow, and F. Grandjean, "A magnetic, neutron diffraction, and Mössbauer spectral study of $Nd_2Fe_{15}Ga_2$ and the $Tb_2Fe_{17-x}Ga_x$ solid solutions," J. Appl. Phys. **76**, 443 (1994).
24. M. Morariu and M. S. Rogalski "^{57}Fe Mössbauer study of $Y_2Fe_{16}M$ compounds and their nitrides with M = Ga, V," Phys. Status Solidi A **141**, 223 (1994).
25. J. M. Cadogan, Hong-Shuo Li, A. Margarian, and J. B. Dunlop, "On the ternary intermetallic phases formed by $YFe_{12-x}Ga_x$ ($1 \leqslant x \leqslant 2$)," Mater. Lett. **18**, 39 (1993).
26. Hong-Shuo Li, Suharyana, J. M. Cadogan, Bo-Ping Ju, Bao-Gen Shen, Fang-Wei Wang, and Wen-Shan Zhan, "A Mossbauer study of $Sm_2Fe_{14}Ga_3C_x$ (x=0-2.5)," IEEE Trans. Mag. **31**, 3716 (1995),
27. M. Z. Huang and W.Y. Ching, "Effects of Al substitution in Nd_2Fe_{17} studied by first principles calculations", J. Appl. Phys. **76**, 7046 (1994).
28. M. Z. Huang. and W.Y. Ching "First principles calculation of the electronic and magnetic properties of $Nd_2Fe_{17-x}M_x$ (M = Si, Ga) solid solutions", J. Appl. Phys. **79**, 5546 (1996).
29. M. Akai, H. Akai, and J. Kanamori, "Electronic Structure of Impurities in Ferromagnetic Iron. II. 3*d* and 4*d* Impurities", J. Phys. Soc. Jpn. **54**, 4257 (1985).
30. B. Drittler, N. Stefanou, S. Blugel, R. Zeller, and P. H. Dederichs, "Electronic structure and magnetic properties of dilute Fe alloys with transition-metal impurities", Phys. Rev. B **40**, 8203 (1989).
31. S. Mirbt, O. Eriksson, B. Johansson, and H. L. Skriver, "Magnetic coupling in 3*d* transition-metal monolayers and bilayers on bcc (100) iron", Phys. Rev. B **52**, 15070 (1995).
32. Effect of Mn substitution on the volume and magnetic properties of Er_2Fe_{17}, J. L. Wang, M. R. Ibarra, C. Marquina, and B. Garcı´a-Landa, W. X. Li, N. Tang, W. Q. Wang, F. M. Yang, and G. H. Wu, J. Appl. Phys, **92**, 1453 (2002).

33. L. Neél, "Propriétés magnétiques de l'état métallique et énergie d'interaction entre atomes magnétiques" Ann. Phys. (Paris), **5**, 232 (1936).
34. Z.W. Li, A.H. Morrish "Negative exchange interactions and Curie temperatures for Sm_2Fe_{17} and $Sm_2Fe_{17}N_y$", Phys. Rev. B **55**, 3670 (1997).
35 J.N. Dahal, L. Wang, S. R. Mishra, V. V Nguyen, and J. P. Liu, "Synthesis and magnetic properties of $SrFe_{12-x-y}Al_xCo_yO_{19}$ nanocomposites prepared via autocombustion technique," J. Alloy and Comp. **595**, 213 (2014)
36. B. G Shen, Z. H. Cheng, B. Liang, H. Q Guo, J. X. Zhang, H. Y. Gong, F. W. Wang, Q. W. Yan, and W. S Zhan, "Structure and magnetocrystalline anisotropy of $R_2Fe_{17-x}Ga_x$ compounds with higher Ga concentration", Appl. Phys. Lett. **67**, 1621 (1995).
37. M. Valeanu, N. Plugaru, and E. Burzo, "Effect of nitrogenation on the magnetic properties of $Y_2Fe_{17-x}M_x$ compounds, with M = Al, Ga or Si", Solid State Commun. **89**, 519 (1994).
38. R. Srilatha and G. Markandeyulu and V. Murty "Effect of Co on the Magnetic Properties of $YGdFe_{17-x}Co_xGa$", IEEE Trans. Magn. **42**, 917 (2006).
39. J. Friedel, G. Leman, and S. Olszewski, "On the Nature of the Magnetic Couplings in Transitional Metals", J. Appl. Phys Suppl. to Vol **32**, 325S (1961).
40. R. F. Sabirianov and S. S. Jaswal "Electronic structure and magnetism in $Sm_2Fe_{17-x}A_x$ (A=Al, Ga, Si)", J. Appl. Phys. **79**, 5942 (1996).
41. Hong-Shuo Li and J. M. D. Coey, "Handbook of Magnetic Materials" edited by K. H. J. Buschow (Elsevier, Amsterdam, Vol 6, Chap. I, p.1. 1991),
42. W. Y. Ching and Ming-Zhu Huang, ''Band Theoretical Investigation of Curie Temperatures of Modified R_2Fe_{17}-Based Intermetallic Compounds,'' J. Appl. Phys. **79**, 4602 (1996).
43. Bo-Ping Hu, Hong-Shuo Li, Bao-Gen Shen, Fang-Wei Wang, J. M. Cadogan, Wen-Shan Zhan, "A ^{57}Fe Mossbauer study of $Gd_2Fe_{17-x}Ga_xC_2$ (x=0-6)", **79**, 5713 (1996).
44. E. E. Kokorina, M. V. Medvedev and I. A. Nekrasov "ab Initio Exchange Interactions and Magnetic Properties of Intermetallic Compound $Gd_2Fe_{17-x}Ga_x$", Solid State Phenomenon, **168-169**, 196 (2010).
45. Z. H. Cheng, B. G. Shen, B. Liang, J. X. Zhang, F. W. Wang, S. Y. Zhang, J. G. Zhao and W. S. Zhan., "Ga-concentration dependence of magnetocrystalline anisotropy in $Gd_2Fe_{17-x}Ga_x$ Compounds" J. Appl. Phys. **78**, 1385 (1995).

46. G. Pokharel, K. S. Syed Ali, and S. R. Mishra, "Structural, magnetic and Mossbauer studies of Ti doped $Gd_2Fe_{17-x}Ti_x$ and $Gd_2Fe_{16}Ga_{1-x}Ti_x$ ($0 \leq x \leq 1$)", J. Magn. Magn. Mater. **382**, 31 (2015).

47. G. J. Long, S.R. Mishra, O.A. Pringle, Z. Hu, W.B. Yelon, F. Grandjean, D. P. Middleton, and K. H. J. Buschow "A magnetic, neutron diffraction, and Mossbauer spectral study of the $Ce_2Fe_{17-x}Ga_x$ solid solutions", J. Magn. Magn. Mater. **176**, 217 (1997).

48. F. Maruyama, "Exchange interactions in $R_2Fe_{17-x}Ga_x$ (R =Y, Sm, Gd, Tb, Ho and Tm) compounds", J. Solid State Chem. **178,** 3020 (2005).

49. A.Paoluzi and L.Pareti, "Magnetocrystalline anisotropy of Fe and Sm sublattices in Sm_2Fe_{17}: effects of Ti substitution for Fe", J. Mang. Magn. Mater. **189**, 89 (1998).

50. L. Liao, PhD thesis, "Cobalt Site in Iron Rare-earth based compounds, McGill University Montréal, Canada, (1992)".

51. P. C. M. Gubbens, and K. H. J. Buschow, "Magnetic phase transition in Tm_2Fe_{17}" J. Appl. Phys. **44**, 3739 (1973).

52. O. Isnard, D. Hautot, G. J. Long, and F. Grandjean, "A structural, magnetic, and Mössbauer pectral study of $Dy_2Fe_{17}$and its hydrides", J. Appl. Phys. **88**, 2750 (2000).

53. K. H. J. Buschow and J. S. V. Wieringen, "Crystal structure and magnetic properties of cerium-iron compounds", Phys. Status Solidi **42**, 231 (1970).

54. L. M. Levinson, E. Rosenberg, A. Shaulov, and K. Strnat, "Mössbauer Study of Some 2–17 Lanthanide-Iron Compounds", J. Appl. Phys. **41**, 910 (1970).

55. E. E. Alp, A. M. Umarji, S. K. Malik, G. K. Shenoy, M. Q. Huang, E. B. Boltich, and W. E. Wallace, "^{57}Fe Mössbauer studies on Si-substituted Er_2Fe_{17}", J. Magn. Magn. Mater. **68**, 305 (1987).

56. J. L. Wang, S. J. Campbell, O. Tegus, C. Marquina, and M. R. Ibarra, "Magnetovolume effect and magnetic properties of $Dy_2Fe_{17-x}Mn_x$", Phys. Rev. B **75**, 174423 (2007).

57. F. Grandjean, O. Isnard, and G. J. Long, "Magnetic and Mossbauer spectral evidence for the suppression of the magnetic spin reorientation in Tm_2Fe_{17} by deuterium", Phys. Rev. B **65**, 064429 (2002).

58. G. J. Long, O. Isnard, and F. Grandjean, "A Mossbauer spectral study of the magnetic properties of Ho_2Fe_{17} and $Ho_2Fe_{17}D_{3.8}$" J. Appl. Phys. **91**, 1423 (2002).

 doi:10.20944/preprints201810.0075.v1

59. P. C. M. Gubbens, J. H. F. van Apeldoorn, A. M. van der Kraan and K. H. J. Buschow, "Mossbauer effect investigation of Y-Fe compounds", J. Phys. F: Metal Physics, **4**, 921 (1974).

60. S. M. Dubiel, "Relationship between the magnetic hyperfine field and the magnetic moment" J. of Alloy and Compounds, **488**, 18-22 (2009).

61. G. J. Long, O. A. Pringle, F. Grandjean, K. H. J. Buschow, "A Mössbauer effect study of the microscopic magnetic properties of Nd_2Fe_{17} and $Nd_2Fe_{17}N_{2.6}$", J. Appl. Phys. **72**, 4845 (1992).

62. N. A. Halasa, G. De Pasquali and H. G. Drickamer, "High-pressure studies on ferrites", Phys. Rev. B **10**, 154 (1974).

63. H. G. Drickamer and C. W. Frank, "Electronic Transitions and the igh-pressure Chemistry and Physics of Solids" (Chapman and Hall, London, 1973).